Collapses and revivals in the interference between two Bose-Einstein condensates formed in small atomic samples

E. M. Wright
Optical Sciences Center, University of Arizona, Tucson, Arizona 85721

T. Wong, M. J. Collett, S. M. Tan, and D. F. Walls
Department of Physics, University of Auckland, Private Bag 92019, Auckland, New Zealand
(Received 21 November 1996)

We investigate the quantum interference between two Bose-Einstein condensates formed in small atomic samples composed of a few thousand atoms both by imposing Bose broken gauge symmetry from the outset and also using an explicit model of atomic detection. In the former case we show that the macroscopic wave function collapses and revives in time, and we calculate the characteristic times for current experiments. Collapses and revivals are also predicted in the interference between two Bose-Einstein condensates which are initially in Fock states, a relative phase between the condensates being established via atomic detections corresponding to uncertainty in the number difference between them. [S1050-2947(97)08807-0]

PACS number(s): 03.75.Fi, 05.30.Jp, 32.80.Pj, 74.20.De

I. INTRODUCTION

The spectacular observations of Bose-Einstein condensation (BEC) in atomic vapors reported last year [1,2] have opened up new avenues of research into the physical properties and nature of Bose-condensed systems. Recent experimental developments include reports of a new trap capable of holding larger number of atoms and measurements of the condensate fraction and mean-field energy [3], nondirect observation of the development of the condensate [4], measurements of the collective oscillations of the condensate [5–7], and an output coupler for an atomic Bose-Einstein condensate [8]. The measurements of the collective excitations have been found to be in excellent agreement with the theoretical predictions from mean-field theory for condensate fractions near unity [9–12]. Such detailed studies of the collective excitations opens the door to investigating superfluid effects in atomic BECs, and, in particular, the general relation between BEC and superfluidity (see, for example, the article by Huang in Ref. [13]).

In this paper we investigate the interference of two BECs formed in small atomic samples composed of 10^3–10^6 atoms, typical of current experiments. Our motivation for this theoretical investigation is that we previously showed that in small atomic samples the macroscopic wave function exhibits collapses and revivals, the first collapse occurring on a few seconds time scale [14]. In that work the notion of Bose broken symmetry [15] was invoked and the quantum state of the condensate was taken as a wave packet composed of states of fixed number of particles, so that, according to the uncertainty relationship between particle number and phase, the condensate phase can become well defined. The collapse of the macroscopic wave function arises from the fact that, due to many-body interactions, the chemical potential is different for each particle number present in the wave packet, and the revivals are a direct consequence of the discreteness of the particle number [14]. Based on this theory one would naively expect that if two BECs are interfered the visibility of the interference pattern should also exhibit the collapses and revivals, hence providing a direct experimental signature of the effect. However, before jumping to conclusions it is important to note that the notion of Bose broken symmetry is only strictly applicable in the thermodynamic limit, where the system size and the number of particles tend to infinity with the density held constant, so that another approach should be utilized to verify the predicted collapse and revivals. Such an approach, freed from the thermodynamic limit and Bose broken symmetry arguments, has emerged in the last year [16–23]. Javanainen and Yoo [16] first showed that an interference pattern between two condensates, and hence a relative phase between the two condensates, could arise from an explicit model of atomic detections: As atomic detections are performed an uncertainty in the number of atoms in each condensate is built up, since we do not know which condensate any atom is removed from. The uncertainty relationship between the relative atom number of the condensates and the relative phase then allows a well defined relative phase to emerge.

The remainder of this paper is organized as follows: Sec. II gives the basic theory for BEC in a trapped gas of atoms as described by the Gross-Pitaevskii equation and within the Thomas-Fermi approximation. The interference between two condensates using the notion of Bose broken symmetry is described in Sec. III, and the collapse and revival times for the macroscopic wave function are evaluated for current experimental conditions. In Sec. IV we approach the interference of two condensates using a quantum anharmonic-oscillator approximation to the full field-theoretical model of Sec. II, and the atomic detection scheme of Ref. [16]. Here we verify that the collapse and revivals are still present without explicitly invoking Bose broken symmetry. In Sec. V we briefly discuss the quantum anharmonic-oscillator model for condensates described by coherent states, i.e., assuming Bose broken symmetry, and demonstrate that the details of the collapses and revivals depends on the quantum state of the condensate. Finally, Sec. VI gives our summary and conclusions.

II. BASIC THEORY

In this section we introduce the second-quantized Hamiltonian for BEC in a trapped gas of atoms, and then discuss the Gross-Pitaevskii equation for the macroscopic wave function and the Thomas-Fermi approximation. Although these topics are amply covered elsewhere we include them for completeness and to clarify our notation.

A. Second-quantized Hamiltonian

Our starting point is the second-quantized Hamiltonian for a system of bosonic atoms confined in a trap potential [24]

$$\hat{H}(t)=\int d\mathbf{r}\left[\frac{\hbar^2}{2m}\nabla\hat{\psi}^\dagger\cdot\nabla\hat{\psi}+V(\mathbf{r})\psi^\dagger\hat{\psi}+\frac{U_0}{2}\hat{\psi}^\dagger\hat{\psi}^\dagger\hat{\psi}\hat{\psi}\right], \tag{1}$$

where $\hat{\psi}(\mathbf{r},t)$ and $\hat{\psi}^\dagger(\mathbf{r},t)$ are the Heisenberg picture field operators which annihilate and create atoms at position $\mathbf{r}$, and obey the equal-time commutation relation $[\hat{\psi}(\mathbf{r},t),\hat{\psi}^\dagger(\mathbf{r}',t)]=\delta(\mathbf{r}-\mathbf{r}')$ appropriate to bosons, the (single-particle) trap potential is taken of the form [25–27]

$$V(\mathbf{r})=\tfrac{1}{2}m(\omega_\perp^0)^2(r_\perp^2+\lambda^2z^2), \tag{2}$$

with $\mathbf{r}=(\mathbf{r}_\perp,z),\mathbf{r}_\perp$ being the transverse position coordinate assuming cylindrical symmetry of the trap potential in the transverse plane, and z the longitudinal coordinate, m is the atomic mass, $\omega_\perp^0$ the transverse angular frequency of the trap, $\lambda=\omega_z^0/\omega_\perp^0$ is the ratio of the longitudinal to transverse frequencies, and $U_0=4\pi\hbar^2a/m$ measures the strength of the two-body interaction, a being the s-wave scattering length. Here we consider a repulsive interaction so that $a>0$.

B. Gross-Pitaevskii equation

Here we consider the standard treatment of the condensate in a Bose gas [28]. At zero temperature, and for a weakly interacting gas, the particles may be assumed to be predominantly in the condensate. The assumption of zero temperature is not too restrictive since atomic condensates can be prepared with condensate fractions close to unity [5,6]. The Schrödinger equation for the state vector of the system is

$$i\hbar\frac{\partial}{\partial t}|\Psi(t)\rangle=\hat{H}(0)|\Psi(t)\rangle, \tag{3}$$

and in the time-dependent Hartree approximation [29–31] the state vector for a system of N particles is written as

$$|\Psi(t)\rangle=(N!)^{-1/2}\left[\int d\mathbf{r}\ \psi_N(\mathbf{r},t)\hat{\psi}^\dagger(\mathbf{r},0)\right]^N|0\rangle, \tag{4}$$

where $\psi_N(\mathbf{r},t)$ is the normalized single-particle wave function, and $|0\rangle$ the vacuum state. Then proceeding in the usual manner [30,31] from the Schrödinger equation (3) we obtain the self-consistent nonlinear Schrödinger equation or Gross-Pitaevskii equation [28] generalized to include the magneto-optical harmonic trap [25–27]

$$i\hbar\frac{\partial\psi_N}{\partial t}=\left[-\frac{\hbar^2}{2m}\nabla^2+\frac{1}{2}m(\omega_\perp^0)^2(r_\perp^2+\lambda^2z^2)+NU_0|\psi_N|^2\right]\psi_N. \tag{5}$$

We are interested in the ground-state solution of this equation for which we set $\psi_N(\mathbf{r},t)=\exp(-i\mu_Nt/\hbar)\phi_N(\mathbf{r})$, giving the stationary Gross-Pitaevskii equation

$$\mu_N\phi_N=\left[-\frac{\hbar^2}{2m}\nabla^2+\frac{1}{2}m(\omega_\perp^0)^2(r_\perp^2+\lambda^2z^2)+NU_0|\phi_N|^2\right]\phi_N, \tag{6}$$

where the macroscopic wave function $\phi_N(\mathbf{r})$ for the N-particle system is normalized to unity. The ground-state energy of the system of N atoms is derived from the Ginzburg-Pitaevskii-Gross energy functional [32]

$$\mathcal{E}_N=N\int d\mathbf{r}\left[\frac{\hbar^2}{2m}|\nabla\phi_N|^2+V(\mathbf{r})|\phi_N|^2+\frac{NU_0}{2}|\phi_N|^4\right], \tag{7}$$

and the parameter μ_N is given by $\mu_N=d\mathcal{E}_N/dN$. By a slight extension of the usual terminology μ_N will be called the chemical potential of the N-particle condensate. The stationary Gross-Pitaevskii equation follows from the variational principle $\delta(\mathcal{E}_N-N\mu_N\int d\mathbf{r}|\phi_N|^2)=0$, and using this we find the further exact result

$$\mu_N'=\frac{d\mu_N}{dN}=U_0\int d\mathbf{r}|\phi_N|^4+\frac{NU_0}{2}\int d\mathbf{r}\frac{\partial}{\partial N}|\phi_N|^4, \tag{8}$$

which can be rearranged to yield

$$U_0\int d\mathbf{r}|\phi_N|^4=\left(1+\frac{N}{2}\frac{\partial}{\partial N}\right)^{-1}\mu_N', \tag{9}$$

which we shall use below.

C. Thomas-Fermi approximation

Edwards and Burnett [25], and Ruprecht *et al.* [26] have solved Eq. (6) numerically to obtain both the condensate wave functions and the chemical potentials μ_N as functions of N. Here we follow Baym and Pethick [27] and use the Thomas-Fermi approximation for the macroscopic wave function, in which the kinetic-energy term in the stationary Gross-Pitaevskii equation is neglected. This yields the approximate macroscopic wave function

$$\phi_N(\mathbf{r}_\perp,z)=(NU_0)^{-1/2}\sqrt{\mu_N-(1/2)m(\omega_\perp^0)^2(r_\perp^2+\lambda^2z^2)}, \tag{10}$$

when the argument of the square root is greater than or equal to zero, zero otherwise. Requiring that the macroscopic wave function be normalized to unity yields the expression for the chemical potential

$$\mu_N=\frac{\hbar\omega_\perp^0}{2}\left(\frac{15\lambda Na}{a_\perp}\right)^{2/5}, \tag{11}$$

TABLE I. Collapse and revivals times t_{coll} and $T_{\overline{N}}$ for some current experiments. The numbers in the ''Expt.'' column have the following meaning: (1) ''strong trap'' experiment in Rb from Ref. [1]; (2) ''weak trap'' experiment in Rb from Ref. [1]; (3) experiment in Rb from Ref. [5]; (4) experiment in Na from Ref. [4].

Expt.	$\omega_\perp^0$ (rad s^{-1})	λ	a (nm)	$\overline{N}$	ζ	t_{coll} (ms)	$T_{\overline{N}}$(s)
1	471	2.8	5.2	2000	0.1	21	6
2	51	2.8	5.2	2000	0.15	320	86
3	828	2.8	5.2	4500	0.06	12	4.9
4	2010	0.056	4.9	5×10^6	0.02	51	710

where $a_\perp=(\hbar/m\omega_\perp^0)^{1/2}$ is the characteristic transverse length scale of the linear potential. The Thomas-Fermi approximation is valid if the coherence length $r_{coh}=(8\pi an)^{-1/2}$ [28], n being the mean density, is less than the characteristic size r_N of the atomic cloud. Following Baym and Pethick [27] we find that

$$\zeta=\frac{r_{coh}}{r_N}=\left(\frac{15\lambda Na}{a_\perp}\right)^{-2/5}, \tag{12}$$

which should be much less than unity for the Thomas-Fermi approximation to apply. In the first four columns of Table I we show the values of the parameters for some current experiments with a positive scattering length, and the fifth column shows the corresponding values of ζ, and we see that the Thomas-Fermi theory should be valid in all cases.

The explicit form of the chemical potential in Eq. (11) can be used to evaluate the overlap integral in Eq. (9) giving

$$U_0\int d\mathbf{r}|\phi_N|^4=\frac{10}{7}\mu_N', \tag{13}$$

a result we shall use later.

III. QUANTUM INTERFERENCE WITH BOSE BROKEN SYMMETRY

In this section we investigate quantum interference between two BECs using the notion of Bose broken gauge symmetry [15]. According to this notion the macroscopic wave function for each condensate attains a fixed but arbitrary phase as a result of the spontaneous breaking of $U(1)$ gauge symmetry during the condensation process. The $U(1)$ gauge symmetry is associated with particle number conservation, so that in the condensed system the particle number is not fixed. Then, as a result of the number-phase uncertainty relationship $\Delta N\Delta\eta\approx1$, the phase η need not be indeterminate, and interference between two BECs is possible. Here we employ a description of the condensate state vector as a wave packet of states of fixed particle number N in the condensate to apply the notion of Bose broken gauge symmetry. In contrast, in Sec. IV we will show atomic detections establish a coherent wave packet without the need to build in Bose broken symmetry from the outset.

A. Wave-packet description

The definition of the macroscopic wave function given in the last section is rigorous in the thermodynamic limit [28]. To investigate the case of a small condensate, say a few thousand atoms, we employ a wave-packet description. In particular, the wave-packet description is intended to reflect the quantum coherence of the condensate for measurement times short compared to relaxation times [22,33]. In contrast, for measurements performed over times long compared to relaxation times, the quantum coherence of the condensate is destroyed and the macroscopic wave function vanishes.

Here we employ a wave packet composed of states of a fixed number of particles N in the condensate, with expansion coefficients $a_N=|a_N|e^{i\zeta_N}$, hence retaining quantum coherence. The present description of BEC, due to Barnett, Burnett, and Vaccarro [22], is therefore different from the conventional η ensemble which employs a wave packet of states corresponding to a different total number of particles, condensate plus noncondensate, and is generally only applicable in the thermodynamic limit [33]. A coherent state with $a_N=\overline{N}^{N/2}e^{iN\eta}e^{-\overline{N}/2}/\sqrt{N!}$ suggests itself, but the states associated with BEC do not generally possess such complete phase coherence [34]. Nevertheless, a pure state description of the condensate may be rendered plausible as follows: Below the Einstein condensation temperature the many-body ground state of the system becomes macroscopically occupied, yielding a condensate which should be considered an open quantum system in contact via many-body interactions with the environment or reservoir composed of the noncondensate atoms. It is known from the work of Zurek, Habib, and Paz [35] and Gallis [36], that for a system, in their case a harmonic oscillator, in interaction with an environment, certain pure states show considerable stability against loss of quantum coherence, and that in the weak-coupling limit the pure states of maximal stability are the coherent states. Thus, the quantum coherence of the condensate may be reasonably represented by a pure state, though perhaps not precisely a coherent state since weak coupling may not hold. This argument does not depend on the size of the system, except that the noncondensate atoms may be viewed as a reservoir, and the conclusions therefore apply even for small condensates far removed from the thermodynamic limit.

We further assume that the particle number distribution $|a_N|^2$ is sharply peaked with variance ΔN around a mean particle number $\overline{N}$. As a concrete example we take a Poissonian distribution for which $\Delta N=\overline{N}^{1/2}$, which is reasonable since the number distribution $|a_N|^2$ of the condensate should be approximately that of a coherent state, though the phases ζ_N may not be so correlated. Under these conditions we may expand the chemical potential μ_N around the mean number $\overline{N}$ in a Taylor series

$$\mu_N = \mu_{\overline{N}} + (N-\overline{N})\mu'_{\overline{N}} + \tfrac{1}{2}(N-\overline{N})^2\mu''_{\overline{N}} + \cdots, \qquad (14)$$

where

$$\mu'_{\overline{N}} = \frac{3}{5}\hbar\omega_\perp^0\left(\frac{\lambda a}{a_\perp}\right)^{2/5}\frac{1}{\overline{N}^{3/5}}. \qquad (15)$$

If we compute the ratio of the third term to the second term in this expansion for $N=\overline{N}+\Delta N$, then we find that the magnitude of this ratio varies as $\overline{N}^{-1/2}$. Thus, even for a low particle number $\overline{N}=10^3$ the second term in the expansion is the dominant correction. In the remainder of this paper we shall, therefore, only retain the first two terms in the above expansion.

B. Condensate state vector

We are now equipped to construct the wave packet for the condensate state vector, which we write as

$$|\Psi(t)\rangle = \sum_N a_N e^{-iN\mu_N t/\hbar}(N!)^{-1/2}(\hat{a}^\dagger)^N|0\rangle, \qquad (16)$$

where the exponential contains the term $N\mu_N$ since there are N particles each of chemical potential μ_N, the operator $\hat{a}^\dagger = \int d^3\mathbf{r}\phi_{\overline{N}}(\mathbf{r})\hat{\psi}^\dagger(\mathbf{r},0)$ creates particles with distribution $\phi_{\overline{N}}(\mathbf{r})$ [24], with $[\hat{a},\hat{a}^\dagger]=1$, and $|0\rangle$ is the vacuum state. The approximations employed in Eq. (16) are tantamount to the Hartree approximation. In general the Schrödinger field annihilation operator can be written as a mode expansion over single-particle states as

$$\hat{\psi}(\mathbf{r},0) = \sum_\alpha \hat{a}_\alpha\varphi_\alpha(\mathbf{r}) = \hat{a}\,\phi_{\overline{N}}(\mathbf{r}) + \tilde{\psi}(\mathbf{r},0), \qquad (17)$$

where $\{\varphi_\alpha(\mathbf{r})\}$ are a complete orthonormal basis set. Here in the last line we have chosen $\varphi_0(\mathbf{r})=\phi_{\overline{N}}(\mathbf{r})$ as one member of the complete orthonormal set, and identified $\hat{a}=\hat{a}_0$. Then by construction the first term in the mode expansion acts only on the condensate state vector, whereas the second term $\tilde{\psi}(\mathbf{r},0)$ accounts for the noncondensate atoms.

C. Collapses and revivals

The state vector (16) may be used to calculate quantum expectation values of the condensate. Of interest to us here are the one-particle reduced density matrix representing the condensate

$$\rho_1(\mathbf{r},\mathbf{r}',t) = \langle\Psi(t)|\hat{b}^\dagger\hat{b}|\Psi(t)\rangle\phi^*_{\overline{N}}(\mathbf{r})\phi_{\overline{N}}(\mathbf{r}') = \overline{N}\phi^*_{\overline{N}}(\mathbf{r})\phi_{\overline{N}}(\mathbf{r}'), \qquad (18)$$

and the macroscopic wave function

$$\langle\hat{\psi}(\mathbf{r},t)\rangle = \langle\Psi(t)|\hat{b}|\Psi(t)\rangle\phi_{\overline{N}}(\mathbf{r}) = \overline{N}^{1/2}\phi_{\overline{N}}(\mathbf{r})e^{-i\mu t/\hbar}\mathcal{F}_{\overline{N}}(t), \qquad (19)$$

where

$$\mathcal{F}_{\overline{N}}(t) = \sum_N \left(\frac{N}{\overline{N}}\right)^{1/2} a^*_{N-1}a_N[\cos(2\mu'_{\overline{N}}(N-\overline{N})t/\hbar) - i\sin(2\mu'_{\overline{N}}(N-\overline{N})t/\hbar)], \qquad (20)$$

and $\mu=\mu_{\overline{N}}+\overline{N}\mu'_{\overline{N}}$ is the net chemical potential of the condensate. Using Eq. (11) for the chemical potential μ_N in the Thomas-Fermi approximation we obtain $\mu=\frac{7}{5}\mu_{\overline{N}}=\mathcal{E}_{\overline{N}}/\overline{N}$, and the net chemical potential μ is equal to the mean energy per particle [27]. In obtaining these results we have used the first two terms in the expansion of the chemical potential (14). The one-particle reduced density matrix (18) is of the classic factorized form representing the off-diagonal long-range order (ODLRO) associated with BEC [37,38]. This conclusion holds for any mean particle number, as long as the mean-field approximations employed are valid. Here the ODLRO extends over separations $|\mathbf{r}-\mathbf{r}'|\approx r_{\overline{N}}$, the spatial scale of the condensate. In the experiments the one-particle reduced density matrix is not measured but rather the momentum space (velocity) distribution is obtained by releasing the atoms from the trap, letting them fall under gravity, and imaging them. The momentum spread will then be $\Delta K\approx 2\pi/r_{\overline{N}}$, so that the ODLRO is transferred to a sharp spike in the imaged atomic distribution [1,2].

Turning now to the macroscopic wave function (19), we see that the factor $\mathcal{F}_{\overline{N}}(t)$ takes the form of a weighted sum of trigonometric functions with different frequencies. Such sums are well known from the Jaynes-Cummings model of quantum optics, which describes the interaction between a single-mode radiation field and a two-level atom, and give rise to the phenomenon of collapses and revivals [39], and the same is expected here. Collapse and revivals also appear in the relative phase between two superfluids or superconductors [40]. Directly from the form of Eq. (20) we see that $|\mathcal{F}_{\overline{N}}(t)|$ is periodic in time with period

$$T_{\overline{N}} = \pi\hbar/\mu'_{\overline{N}}, \qquad (21)$$

and the revivals occur with this period. The revivals result from the fact that the sum in Eq. (20) is over the discrete particle number, so that they are a direct result of the granularity of matter. The collapses depend on the choice of the number distribution $|a_N|^2$. For our purposes we only need the variance ΔN in particle number and the assumption that the phases are correlated enough that $\mathcal{F}_{\overline{N}}(0)$ does not vanish exactly. Then $\mathcal{F}_{\overline{N}}(t)$ is periodic and has a maximum in magnitude at $t=t_{max}$. At this time the net phases for each N are such that they add most constructively in the sum in Eq. (20). As time increases these phase relations will initially be lost thus producing a collapse of the magnitude of $\mathcal{F}_{\overline{N}}(t)\to 0$, until the system revives at $t=t_{max}+T_{\overline{N}}$. The collapse time t_{coll} may be estimated by looking at the spread of frequencies present in the wave packet for particle numbers between $N=\overline{N}\pm\Delta N/2$, which yields $\Delta\Omega=2\mu'_{\overline{N}}\Delta N/\hbar$, and $t_{coll}\geqslant 1/\Delta\Omega$. Gathering our results together for the collapse and revival times we have

$$T_{\overline{N}} \approx \frac{5}{\omega_\perp^0}\left(\frac{a_\perp}{\lambda a}\right)^{2/5}\overline{N}^{3/5}, \quad t_{coll} \geqslant \frac{T_{\overline{N}}}{2\pi\Delta N}. \qquad (22)$$

In particular, if we evaluate Eq. (20) for a coherent state with $\overline{N} \gg 1, \Delta N = \overline{N^{1/2}}$, we find $|\mathcal{F}_{\overline{N}}(t)|^2 = \exp(-t^2/t_{coll}^2)$, with t_{coll} given by the equality in Eq. (22). Thus, a coherent state gives rise to the minimum collapse time for a Poissonian distribution.

The collapse phenomenon actually occurs under far more general conditions than reflected by the approximations used here, the essential ingredient being dispersion of the chemical potential μ_N over the particle number variance ΔN. Landau damping of plasma oscillations in an electron plasma is another example of decay of a coherent state. In contrast, the exactly periodic revivals arise from the linear dependence of μ_N on $(N-\overline{N})$ employed in Eq. (14). If higher-order corrections are retained in the expansion (14) the revivals are no longer perfectly periodic, and diminish with increasing time. We also note that according to Eq. (18) the single-particle reduced density matrix is insensitive to the collapse and revivals of the macroscopic wave function, which is then also the case for the atomic BEC experiments [1,2].

D. Thermodynamic limit

The thermodynamic limit of these results must be taken with care. In particular, in order to maintain a constant density as the mean particle number is increased it is necessary to concomitantly increase the linear trap size as $r_t \propto \overline{N^{1/6}}$. Then $T_{\overline{N}} \propto \overline{N}$ and $t_{coll} \propto \overline{N^{1/2}}$, so that collapse and revivals become irrelevant for $\overline{N} \to \infty$. In addition, we find that $\mathcal{F}_{\overline{N}}(0) \to e^{i\eta}$ by the following argument: The approximate uncertainty relation $\Delta N \Delta \eta \approx 1$ holds for the number and phase fluctuations of the condensate. Then, as $\Delta N = \overline{N^{1/2}} \to \infty$ we have $\Delta \eta \to 0$, which is the case for a coherent state with phases $\zeta_N = N\eta$. Thus, in the thermodynamic limit the quantum state of the condensate approaches a coherent state for which we find $\mathcal{F}_{\overline{N}}(0) = e^{i\eta}$. We then have $\langle \hat{\psi}(\mathbf{r},t) \rangle = e^{i\eta} \overline{N^{1/2}} \phi_{\overline{N}}(\mathbf{r}) e^{-i\mu t/\hbar}$, and this is precisely the limit in which the macroscopic wave function acts as an order parameter [28].

E. Interference between two condensates

We now consider the case that the atomic BEC is interfered with a second large condensate whose macroscopic wave function we write as $C\exp[i(\mathbf{k}\cdot\mathbf{r} - \mu t/\hbar + \chi)]$. Here we have assumed that the second condensate is spatially large and write it as a plane wave with wave vector $\mathbf{k}$, and has the same chemical potential as the first for simplicity. We further assume that the second condensate is composed of a large number of atoms so that collapses and revivals are not an issue, the constant C is real, and χ is the arbitrary but fixed phase of the condensate. Then, when the two condensates are made to interfere, say by dropping them on top of each other, the resulting interference pattern is described by the cross term

$$\mathcal{I}(\mathbf{r},t) = C\langle \hat{\psi}(\mathbf{r},t) e^{-i(\mathbf{k}\cdot\mathbf{r}+\chi)} + \hat{\psi}^\dagger(\mathbf{r},t) e^{i(\mathbf{k}\cdot\mathbf{r}+\chi)} \rangle$$
$$= 2C\overline{N^{1/2}} \phi_{\overline{N}}(\mathbf{r}) |\mathcal{F}_{\overline{N}}(t)| \cos[\mathbf{k}\cdot\mathbf{r} + \chi - \arg(\mathcal{F}_{\overline{N}}(t))]. \tag{23}$$

In the thermodynamic limit where $\mathcal{F}_{\overline{N}}(t) \to e^{i\eta}$ this interference pattern takes the form of a stationary spatial modulation of wave vector $\mathbf{k}$ over the spatial extent $r_{\overline{N}}$ of the condensate (we assume $|\mathbf{k}| r_{\overline{N}} \gg 1$ so that an interference pattern is evident). However, due to the factor $|\mathcal{F}_{\overline{N}}(t)|$ appearing in the interference pattern it is clear that the interference will display the collapses and revivals predicted for the macroscopic wave function: when the macroscopic wave function collapses and revives so does the visibility of the interference pattern with the same period $T_{\overline{N}}$.

Thus quantum interference of two condensates provides an experimental signature of the predicted collapses and revivals. Furthermore, the arguments are easily extended to the case that both condensates display collapses and revivals, that is two identical condensates, and the same conclusions apply.

F. Experimental parameters

The collapse and revival times calculated for the current experiments are shown in columns six and seven of Table I, respectively. The collapse times quoted are the minimum values derived from Eq. (22), that is for coherent states. Here we see that the collapse times are all less than 1 s, and well within the condensate lifetimes of 15 s for Rb [1] and 1 s for Na [2], which suggests that collapse of the macroscopic wave function occurs in these traps. In contrast, the revival times are considerably longer. However, the 6 s revival time found for the strong trap in Rb is still within the condensate lifetime of 15 s quoted for that experiment [1], though the effects of dissipation may quench the revival. In this respect, we note that the recent Rb experiment (third row) with a higher trap frequency and mean particle number has a lower revival time of 3.75 s.

IV. QUANTUM PHASE FROM MEASUREMENTS

In this section we look at the buildup of quantum coherence between two Bose-Einstein condensates initially in Fock states. Since we start from Fock states no phase is initially assumed with a phase only established via the measurement process. The system we consider was first proposed by Javanainen and Yoo [16], and consists of two Bose-Einstein condensates which are dropped on top of one another. Each of the condensates consist of n atoms with momentum k_1 and k_2 directed along the x axis, respectively. Atoms are detected on a screen placed below the two condensates. A detection at some position x is represented by the field operator for the sum of the two condensates

$$\hat{\Psi}(x) = \frac{1}{\sqrt{2}} (\hat{a}_1 + \hat{a}_2 e^{i\phi(x)}), \tag{24}$$

where $\phi(x) = (k_2 - k_1)x$, and $\hat{a}_1$ and $\hat{a}_2$ are the atom annihilation operators for the first and second Bose-Einstein condensates, respectively, (see below). An interference pattern is generated from the two condensates because every detection of an atom introduces uncertainty into the atom number in each condensate since we do not know which condensate this atom came from. However, the total number in both condensates is always known since it is just the initial total number minus the number of detections we have observed. The un-

certainty relationship between the relative atom number and phase between these condensates allows us to establish a relative phase between them to some precision.

The effect of collisions on the establishment of quantum phase has been studied previously [20]. Here we extend this work to demonstrate collapses and revivals in the visibility pattern between two interfering condensates.

A. Single-mode approximation

For the purposes of developing a model based on atomic detection the full quantum-field theory involving the field operators is cumbersome. Thus, here we reduce the full problem by using a mode expansion and truncating. In particular, we write the Heisenberg field annihilation operator as a mode expansion over single-particle states as

$$\hat{\psi}(\mathbf{r},t)=\sum_{\alpha}\ \hat{a}_{\alpha}(t)\varphi_{\alpha}(\mathbf{r})=\hat{a}(t)\phi_{\overline{N}}(\mathbf{r})+\tilde{\psi}(\mathbf{r},t), \quad (25)$$

where $\{\varphi_{\alpha}(\mathbf{r})\}$ are a complete orthonormal basis set. Here, in the last line, we have chosen $\varphi_0(\mathbf{r})=\phi_{\overline{N}}(\mathbf{r})$ as one member of the complete orthonormal set, and identified $\hat{a}=\hat{a}_0$. Then by construction the first term in the mode expansion acts only on the condensate state vector, whereas the second term $\tilde{\psi}(\mathbf{r},t)$ accounts for the noncondensate atoms. Then substituting the mode expansion in the second-quantized Hamiltonian (1), retaining only the first term representing the condensate, and using the Gross-Pitaevskii Eq. (6), we obtain the following single-mode quantum Hamiltonian for the condensate in the Schrödinger picture:

$$\hat{H}_S=\hat{H}(0)=\hat{a}^{\dagger}\hat{a}e_{\overline{N}}+\frac{\hbar\kappa}{2}\hat{a}^{\dagger}\hat{a}^{\dagger}\hat{a}\hat{a}, \quad (26)$$

where

$$\hbar\kappa=U_0\int d\mathbf{r}|\phi_{\overline{N}}|^4, \quad (27)$$

which using Eq. (13) yields $\hbar\kappa=\frac{10}{7}\mu'_{\overline{N}}$, κ being the collision rate between condensate atoms. The first term on the right-hand side, which gives rise to an energy shift, is the number operator $\hat{a}^{\dagger}\hat{a}$ times the single-particle contribution to the energy per particle,

$$e_{\overline{N}}=\int d\mathbf{r}\left[\frac{\hbar^2}{2m}|\nabla\phi_{\overline{N}}|^2+V(\mathbf{r})|\phi_{\overline{N}}|^2\right], \quad (28)$$

whereas the second term accounts for many-body interactions. To proceed we introduce an interaction picture defined by the transformation

$$\hat{H}_I(t)=\hat{U}^{\dagger}(t)\left[\hat{H}_S-i\hbar\frac{\partial\hat{U}(t)}{\partial t}\right]\hat{U}(t),$$

$$\hat{U}(t)=e^{-i(e_{\overline{N}}-\hbar\kappa/2)\hat{a}^{\dagger}\hat{a}t/\hbar}. \quad (29)$$

which yields the single-mode Hamiltonian

$$\hat{H}(t)=\frac{\hbar\kappa}{2}(\hat{a}^{\dagger}\hat{a})^2, \quad (30)$$

where we have dropped the subscript I on the interaction picture operators for simplicity in notation. In the following sections we shall use this single-mode Hamiltonian, which is that of a quantum anharmonic oscillator, as a model for an individual atomic BEC.

A basic assumption underlying this model is that the quantum state describing the condensate involves only particle numbers $n\approx\overline{N}$, that is the particle number remains close to the mean number. The single-mode Hamiltonian (30) gives rise to a particle number dependent phase shift $\chi_N=\kappa N=\frac{10}{7}\mu'_N N/\hbar$ (see Sec. V). However, Eq. (20) reveals a particle number dependent phase shift $\chi_N=2\mu'_N N/\hbar$. The discrepancy between these two results arises since the phase shift in the single-mode theory is an average over the spatial profile of the macroscopic wave function, as evidenced by the overlap integral in the definition of the collision rate κ in Eq. (27). This averaged value is less than the peak value of the actual phase shift which appears in expression (20). In the following we shall replace the factor $\frac{10}{7}$ by 2 in the definition of κ

$$\hbar\kappa=2\mu'_N, \quad (31)$$

so that the correct phase shift is produced by the quantum anharmonic-oscillator model. This relation provides the connection between the single-mode theory parameters and those obtained from the treatment based on the Gross-Pitaevskii equation.

In general we shall consider two interfering condensates. For the ith condensate described by single-mode operators $\hat{a}_i,\hat{a}_i^{\dagger}$ we assign a wave vector k_i, directed along the x axis for simplicity, so that the interference between the condensates can be discussed. The resulting interference pattern would be further modulated by the detailed spatial structure of each condensate, as determined by the solution of the Gross-Pitaevskii equation, but this is of secondary importance and we do not discuss it here. In general, we assume that any interference is well resolved within the spatial extent of the condensates.

B. Effect of collisions

The effect of collisions can be numerically simulated via a Monte Carlo wave function method. The Monte Carlo method is used to simulate both the detection process of rate γ (as quantum jumps) and the time evolutions between detections (as evolution of the wave function between the jumps). The initial Fock state, say $|n,n\rangle$, becomes an expansion of $m+1$ entangled Fock states after m detections. Let us write the state vector after m detections as

$$|\varphi_m\rangle=\sum_{k=0}^{m}c_k|n-m+k,n-k\rangle, \quad (32)$$

which is normalized so that $\Sigma|c_k|^2=1$. The effects of the collisions are included in the time evolution operator for the two condensates

$$\hat{\mathcal{U}}(t)=e^{-i(\hat{H}_1+\hat{H}_2)t/\hbar}=\exp\left(-\frac{i\kappa}{2}[(\hat{a}_1^\dagger\hat{a}_1)^2+(\hat{a}_2^\dagger\hat{a}_2)^2]t\right), \tag{33}$$

with $\hat{H}_i$ the Hamiltonian for the ith condensate. Thus after m detections we have prepared a state $|\varphi_m\rangle$ which then experiences the above evolution operator for a time t followed by a further detection. The conditional visibility of this detection is

$$p(x|x_1,\ldots,x_m,t)\propto\langle\varphi_m|\hat{\mathcal{U}}^\dagger(t)\hat{\Psi}^\dagger(x)\hat{\Psi}(x)\hat{\mathcal{U}}(t)|\varphi_m\rangle. \tag{34}$$

The expectation value for the total number operator is

$$\langle\varphi_m|\hat{\mathcal{U}}^\dagger(t)(\hat{a}_1^\dagger\hat{a}_1+\hat{a}_2^\dagger\hat{a}_2)\hat{\mathcal{U}}(t)|\varphi_m\rangle=2n-m, \tag{35}$$

and, as expected, it is just the total initial number of atoms minus the number of detections. The expectation value of the cross term which gives the size of the conditional visibility is

$$\begin{aligned}\langle\varphi_m|\hat{\mathcal{U}}^\dagger(t)\hat{a}_1^\dagger\hat{a}_2\hat{\mathcal{U}}(t)|\varphi_m\rangle e^{i\phi(x)}&\\ =\sum_{k=1}^{m}c_k^*c_{k-1}\sqrt{(n-k+1)(n-m+k)}&\\ \times\exp\{i\kappa t[2k-(m+1)+i\phi(x)]\}.&\end{aligned} \tag{36}$$

Putting Eqs. (35) and (36) into Eq. (34) we obtain

$$\begin{aligned}p(x|x_1,\ldots,x_m,t)\propto n-m/2+\sum_{k=1}^{m}\mathcal{A}(k)\cos[\phi(x)&\\ +\kappa t(2k-m-1)-\Theta_k],&\end{aligned} \tag{37}$$

where we have defined the phase Θ_k from the coefficients of the state vector as $c_k^*c_{k-1}=A_ke^{-i\Theta_k}$ and the weighting function $\mathcal{A}$ is

$$\mathcal{A}(k)=A_k\sqrt{(n-k+1)(n-m+k)}. \tag{38}$$

We take Θ_k outside the summation since it is defined as the relative phase between neighboring number states which we will assume to be fairly constant for large m. As we detect more and more atoms the resulting entangled state approaches something that resembles a coherent state where the relative phase between neighboring number states (in a number state basis) is identical to the phase of this state. Let this fairly constant relative phase be denoted as Θ which is a good estimate of the relative phase between the two condensates. By expanding the cosine terms in Eq. (37) to separate the time dependence from the phase terms, and noting that the resulting summation over sine functions vanishes due to the cancellation of positive and negative frequency components, we obtain

$$\begin{aligned}p(x|x_1,\ldots,x_m,t)\propto n-m/2+\sum_{k=1}^{m}\mathcal{A}(k)&\\ \times\cos[(2k-m-1)\kappa t]\cos[\phi(x)-\Theta].&\end{aligned} \tag{39}$$

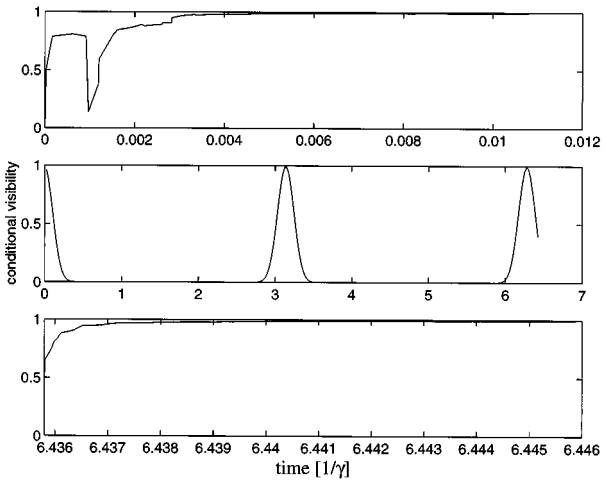

FIG. 1. The top graph shows the growth in the conditional visibility as a function of time corresponding to 100 atomic detections. The middle displays the collapse and revivals of this conditional visibility when the detection process is turned off and the bottom graph shows the growth of this visibility when the detection process is turned on again. The total number of atoms in the two condensates was 10 000 and we have used a collision to detection rate ratio of one ($\kappa=\gamma$) for the initial and final detection periods.

The visibility of the interference pattern is therefore determined from a weighted sum over cosines of differing frequencies. These frequencies depend on the parity of the expression enclosed by the round brackets, $2k-m-1$. When this is odd (m is even) the frequencies are $\{1-m,\ldots,-3,-1,1,3,\ldots,m-1\}$ whereas when it is even (m is odd) they are $\{1-m,\ldots,-2,0,2,\ldots,m-1\}$. In both cases the revival period of the visibility is

$$T=\frac{\pi}{\kappa}=\frac{\pi\hbar}{2\mu'_{\overline{N}}}, \tag{40}$$

with $\overline{N}=n$. This revival period is precisely half that obtained assuming Bose broken symmetry in Sec. III, and this difference shall be taken up in Sec. V. For the case where m is even so that we have a sum over odd frequencies, the cosine term in Eq. (39) alternates between plus or minus 1 at subsequent revival times. Since the visibility is by definition a positive quantity, this alternate sign change in the cosine term represents a π phase shift of the interference pattern at alternate revivals.

For collision to detection rate ratio of one we expect from Eq. (40) a period of π when time is measured in units of the inverse detection rate γ. This agrees very well to the collapse and revival period displayed in the middle graph of Fig. (1). This figure and the π phase shift will be explained in detail in Sec. V.

C. Numerical results

In a numerical simulation the effects of collisions between subsequent detections can be easily modeled with the use of the Monte Carlo wave-function method [41]. We use the following effective Hamiltonian:

$$\hat{H}_{eff}=\frac{\hbar\kappa}{2}[(\hat{a}_1^\dagger\hat{a}_1)^2+(\hat{a}_2^\dagger\hat{a}_2)^2]-\frac{i\hbar\gamma}{2}(\hat{a}_1^\dagger\hat{a}_1+\hat{a}_2^\dagger\hat{a}_2), \tag{41}$$

where the detection and collision rates are γ and κ, respectively. The detections are then turned off and the system undergoes coherent evolution by the Hamiltonian

$$\hat{H}=\frac{\hbar\kappa}{2}[(\hat{a}_1^\dagger\hat{a}_1)^2+(\hat{a}_2^\dagger\hat{a}_2)^2]. \tag{42}$$

We have modeled the collisions that occur only between the atoms of the same condensate. A cross-collision term $(\hat{a}_1^\dagger\hat{a}_1\hat{a}_2^\dagger\hat{a}_2)$ between the condensates is not included. The size of the coefficient of this term depends on the physical geometry of the situation (the overlap of the two condensates) ranging from zero to $\hbar\kappa$. Setting this coefficient to zero we are taking the worst case scenario where the effects of the collisions are the strongest. Alternatively, setting the cross-collision term to $\hbar k$ completes the square in the Hamiltonian so that the subsequent evolution depends only on the total atom number. The effect of the collisions would then be to rotate the phase of the entire state vector, and the coherence between the individual entangled number states would be preserved.

In each run of the numerical simulation the state vector experiences three different regimes. Initially a sequence of detections are accumulated to prepare the entangled state, after which the detections are turned off. During the coherent evolution stage free of detections, the conditional visibility undergoes collapses and revivals due to collisions. Finally, the detections are turned on again. If the detections are turned on when the visibility is zero, during a collapse, it is quickly reestablished by the second sequence of detections. If, however, the detections are turned on when the visibility is in a revival phase the visibility starts from this nonzero value and then quickly increases to one. This behavior is seen in Fig. 1 where the detection process occurs at a much faster rate than the collapse and revivals, and we thus graph the single run on three separate sets of axes: The top graph shows the initial growth of the conditional visibility due to the detections of atoms from the condensates, and the visibility quickly increases to a value close to unity after 100 atoms are detected. (In these simulations the total number of atoms is 10^5 and 200 atomic detections are made, so the assumption underlying the quantum anharmonic-oscillator model that the mean number of atoms varies little is well obeyed.) The middle graph shows what happens to the visibility once the detection process is turned off and the state vector undergoes coherent evolution due to the Hamiltonian in Eq. (42), and collapses and revivals of the visibility are clearly evident. This behavior is reminiscent of the collapses and revivals in the Jaynes-Cummings model of quantum optics for a two-photon process which also displays the periodic revivals of Fig. 1. The bottom graph displays the subsequent evolution of the visibility when the detection process is turned on again. Due to the collapses and revivals during the coherent evolution, the initial visibility for the final stage depends on the time at which the detections are reinitiated. Whatever the initial visibility, this second detection proceeds very rapidly to increase the visibility to a value close to unity.

The cleanliness and exhibition of full revivals in the middle graph of Fig. 1 can be understood by noticing that the two condensate system is a closed system (no loss mechanism) undergoing coherent evolution. The state vector after the initial sequence of detections is an expansion of entangled number states. The effect of collisions during the coherent evolution is to rotate the phase of the coefficients of each entangled state by an amount proportional to the sum of the squares of the number of atoms in each condensate. Thus the phase of the coefficients of this state vector rotate at differing frequencies.

So far we have shown collapses and revivals in the conditional visibility of the interference pattern. For something more relevant to an experimental situation we would like to look at variables associated with the actual observed interference patterns. The phase shift of an interference pattern is a direct measure of the relative phase established between the two condensates. Thus, let us consider the following procedure: Firstly, we prepare a state vector of the two condensates with an established relative phase via measurements, and consider this entangled state between the two condensates after the detections to be our initial state which possesses some degree of coherence. This state is then allowed to undergo coherent evolution with no detections, and finally we turn on the measurement process after an elapsed time and collect our second sequence of measurements. The phase of the resulting interference pattern is calculated with respect to the phase of the interference pattern we observed previously from the first sequence of measurements. Now we reprepare the initial state and repeat the second sequence of measurements and subsequent calculation of phase. Repeating this many times we obtain a set of relative phases between the first and second set of measurements, the idea being that if the time elapsed between the two detection regimes corresponds to some multiple of the full revival time then this set of relative phases should be sharply peaked at zero. For other elapsed times we may expect to see partial revivals. We do not need to numerically calculate the coherent evolution but what we need from the numerical simulation is the coefficients of the prepared state $|\varphi_m\rangle$. Its coherent evolution due to the Hamiltonian $\hat{H}$ describing the collisions previously given by Eq. (42) is

$$\begin{aligned}|\varphi_m(t)\rangle&=\exp(-i\hat{H}t/\hbar)|\varphi_m\rangle\\&=\exp\left(-\frac{i}{2}\kappa[n^2+(n-m)^2]t\right)\\&\quad\times\sum_{k=0}^{m}c_k\exp(-i\kappa[-mk+k^2]t)|n-m+k,n-k\rangle.\end{aligned} \tag{43}$$

We use the phase eigenstates for the atom number difference between the two condensates

$$|\phi\rangle=\sum_{n_1,n_2}\exp\left[-\frac{i}{2}(n_1-n_2)\phi\right]|n_1,n_2\rangle, \tag{44}$$

which has a factor of one-half in the exponential since the state $|\varphi_m\rangle$ has a fixed total atom number of $2n-m$ so that the atom number difference (n_1-n_2) is quantized in units of

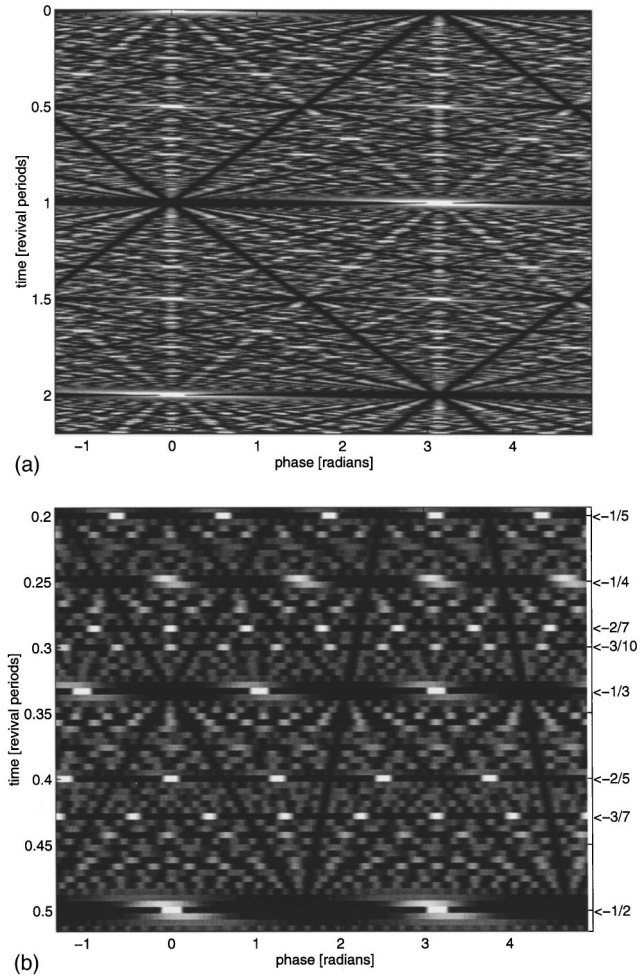

FIG. 2. Plot of the phase distribution when the number of detections (m) is even as a function of the turning on time. The phase is the relative phase between the first and second sequence of measurements in units of radians while the turning on time is in units of the revival period. The brightness of a region corresponds to the relative probability of obtaining a particular phase for a particular turning on time. The bright regions denotes peaks while the darker ones correspond to valleys. The entire plot is shown in (a) with a zoomed in plot between 0.2–0.5 times displayed in (b).

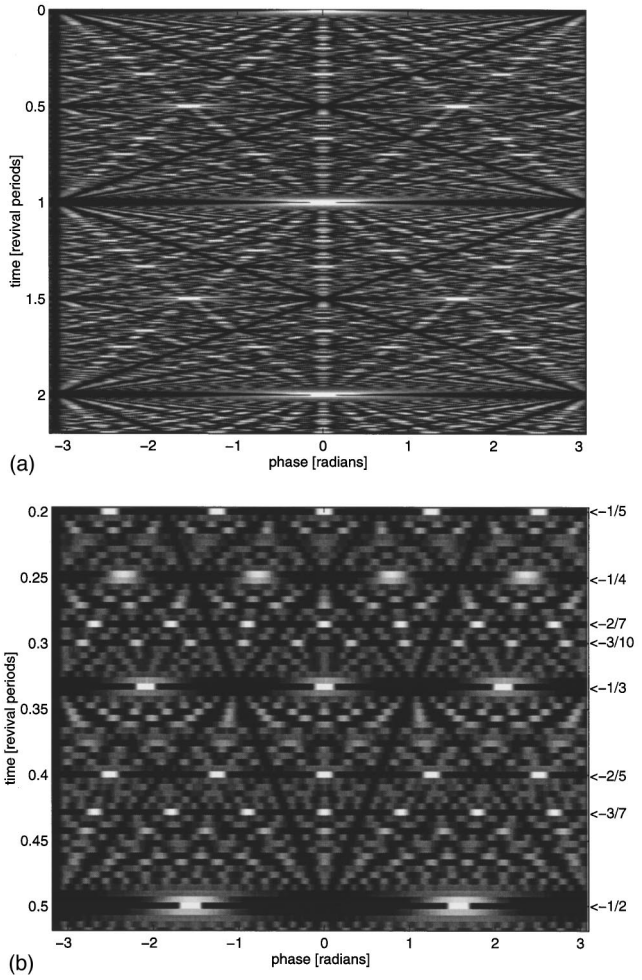

FIG. 3. Plot of the phase distribution when the number of detections (m) is odd as a function of the turning on time. The entire plot is shown in (a) with a zoomed in plot between 0.2–0.5 times displayed in (b).

2. Thus this factor is required so that ϕ is the relative phase between the condensates. The probability distribution of the phase ϕ after elapsed time t is

$$|\langle\phi|\varphi_m(t)\rangle|^2=\left|\sum_{k=0}^{m} c_k\exp(-i[k(k-m)\kappa t+2k\phi])\right|^2. \tag{45}$$

This probability is a function of two variables, phase and elapsed time, and is evaluated numerically. We display the probability distributions in ''birds-eye'' plots via the ''image'' command using MATLAB. Figure 2(a) displays the probability distribution when we have made an even number of detections (m even). The white regions denotes the peaks with the black ones corresponding to the valleys. We see a sharp peak at zero time about zero phase difference between the two interference patterns, this is not surprising since no coherent evolution has occurred. By the time we have evolved for one revival period we obtain a sharp peak at π radians corresponding to the first revival time with π phase shift due to detecting an even number of atoms described in the preceding section. The second revival occurs at a phase difference of zero radians as predicted. Away from these revival times, the phase distribution is not flat but displays many partial revivals. Figure 2(b) is a zoomed in view of Fig. 2(a) between 0.2 and 0.5 revival periods, we can clearly see the partial revival at 0.2 which consists of five peaks. In fact we see partial revivals at every integer fraction of a revival period provided the resolution is good enough. We illustrate this by labeling to the left of the graph with the appropriate integer fractions corresponding to the particular partial revival. Figure 3 shows the distribution for the other case where the number of detections is odd. As predicted there is no π phase shifts. Again, we see partial revivals when we zoom in between 0.2 and 0.5 revival periods as shown in Fig. 3(b).

V. QUANTUM OSCILLATOR MODEL WITH BROKEN SYMMETRY

We will show in this brief section that collapses and revivals also arise for the quantum anharmonic-oscillator

model for initial coherent states instead of preparing an entangled state from an initial detection process. In the language of the preceding section we are considering the interference between two coherent states including the effects of collisions. Thus we treat the Bose-Einstein condensates as coherent states, analogous to the treatment in Sec. III, imposing on them a relative phase whereas previously we establish this phase via measurements.

The Hamiltonian for the two condensates is

$$H=\frac{1}{2}\sum_{i=1}^{2}\hbar\kappa(\hat{a}_i^\dagger\hat{a}_i)^2, \tag{46}$$

giving the Heisenberg equation of motion for each field annihilation operator

$$\frac{d\hat{a}_i}{dt}=\frac{1}{i\hbar}[\hat{a}_i,H]=\frac{\kappa}{2i}(1+2\hat{a}_i^\dagger\hat{a}_i)\hat{a}_i. \tag{47}$$

By inspection the time dependence of the $\hat{a}_i$ operator is

$$\hat{a}_i(t)=\exp\left[-\frac{i}{2}(1+2\hat{a}_i^\dagger\hat{a}_i)\kappa t\right]\hat{a}_i, \tag{48}$$

which yields the Heisenberg picture field operator for the sum of the two modes

$$\hat{\Psi}(t)=\frac{1}{\sqrt{2}}\left\{\exp\left[-\frac{i}{2}(1+2\hat{a}_1^\dagger\hat{a}_1)\kappa t\right]\hat{a}_1 + \exp\left[-\frac{i}{2}(1+2\hat{a}_2^\dagger\hat{a}_2)\kappa t\right]\hat{a}_2\right\}, \tag{49}$$

where we have suppressed the spatial dependence. This yields the operator for the intensity of the atomic pattern as

$$\hat{\Psi}^\dagger(t)\hat{\Psi}(t)=\tfrac{1}{2}\{\hat{a}_1^\dagger\hat{a}_1+\hat{a}_2^\dagger\hat{a}_2+\hat{a}_1^\dagger\exp[i(\hat{a}_1^\dagger\hat{a}_1-\hat{a}_2^\dagger\hat{a}_2)\kappa t]\hat{a}_2 + \text{H.c.}\}. \tag{50}$$

Thus, if we define the initial coherent states as $|\alpha\rangle$ and $|\beta\rangle$ for the modes $\hat{a}_1$and $\hat{a}_2$, respectively, the intensity is evaluated to be

$$\begin{aligned} I\propto&\langle\alpha,\beta|\hat{\Psi}^\dagger(t)\hat{\Psi}(t)|\alpha,\beta\rangle \\ =&\tfrac{1}{2}\{|\alpha|^2+|\beta|^2+\alpha^*\beta\exp[(e^{i\kappa t}-1)|\alpha|^2 \\ &+(e^{-i\kappa t}-1)|\beta|^2]+\beta^*\alpha\exp[(e^{-i\kappa t}-1)|\alpha|^2 \\ &+(e^{i\kappa t}-1)|\beta|^2]\}, \end{aligned} \tag{51}$$

with the aid of the following identity [42]:

$$\langle\alpha|e^{-xa^\dagger a}|\alpha\rangle=\exp[(e^{-x}-1)|\alpha|^2].$$

In the case of maximum visibility of the interference pattern we need the modes to be equal in amplitude, thus we set $\beta=\alpha e^{-i\phi}$, where ϕ is the phase difference between the modes. Substituting this into Eq. (51) we obtain

$$I\propto|\alpha|^2\{1+\exp[2|\alpha|^2(\cos\kappa t-1)]\cos\phi\}. \tag{52}$$

The characteristics of collapses and revivals can be clearly seen in Eq. (52). Revivals occur at times $t=2\pi n/\kappa$ (where n is an integer) with the shape of the collapses described by the exponential term whenever t is no longer a multiple of $2\pi/\kappa$. The period of these revivals is

$$T=\frac{2\pi}{\kappa}=\frac{\pi\hbar}{\mu'_{\overline{N}}}, \tag{53}$$

which is identical to Eq. (21) with $\overline{N}=|\alpha|^2$. This gives twice the period of the previous case of revivals from a detection process [see Eq. (40)], even though we have used identical Hamiltonians. This difference arises because we have two independent coherent states here whereas in the case of detecting atoms from two initial Fock states the total atom number is always fixed at the initial total number minus the number of atomic detections. This additional constraint on the total number means that the difference atom number operator inside the exponential in Eq. (50) is quantized in units of 2. The above expression for the period is only applicable when we are free to superpose total atom numbers, as in the case of two coherent states for which the difference atom number operator is quantized in units of 1. This gives a factor of 2 difference in the revival times between assuming an initial relative phase and establishing this phase in the dynamics of the revivals. The visibility, as described by Eq. (52), smoothly drops to its minimal value halfway between subsequent revivals, exactly where the state induced by detection would have an additional revival.

VI. SUMMARY AND CONCLUSIONS

In this paper we have shown that within the approximation of Bose broken symmetry the macroscopic wave function in small atomic samples exhibits collapse and revivals in time while the BEC is maintained in the form of ODLRO. For current experiments the collapse time is a second or less. The revival time is longer but our results show that it may still fall within the condensate lifetime for some experiments. To detect the collapses and revivals experimentally a scheme is required which is sensitive to the macroscopic wave function directly, and this does not seem to be the case for the coherent light scattering methods previously discussed [43–45]. However, Imamoglu and Kennedy [46] and Javanainen [47] have recently proposed light scattering schemes involving two independent condensates coupled by a common excited state. These schemes rely on the fact that when one condensate is driven optically the light scattered from the other condensate has a nonzero value of the electric field and a phase proportional to the relative phase of the two condensates. By driving both wells and adjusting the phase difference of the fields the scattering can be suppressed via quantum interference, and this in turn determines the phase difference between the two condensates. The scattering is therefore sensitive to Bose broken gauge symmetry. In addition, the light-scattering rate is proportional to the magnitude of the macroscopic wave function, so these schemes could be used to detect the collapses and revivals experimentally. Alternatively, as we have shown here, a direct measurement of the collapse and revivals in the visibility of the interference between two condensates can be made.

In a second approach we have also studied the establishment of a relative phase between two interfering condensates using the explicit measurement model first proposed by Javanainen and Yoo [16]. This model is free from any assumptions concerning Bose broken symmetry or the thermodynamic limit, and is therefore applicable to small atomic samples. In this case we consider the two interfering condensates to be in number states initially, an extreme example for which there is no relative phase before atomic detections. These condensates are then prepared into an entangled state vector composed of entangled number eigenstates via the measurement process. The effects of collisions in the time evolution is to rotate the phases of the individual entangled eigenstates of the state vector. We observe the collapse and revivals of this state under coherent evolution when the measurement process is turned off. Accurate predictions of the period of these collapses and revivals were obtained. The simple anharmonic model of interference between two condensates also displays collapses and revivals. The period of these revivals is twice the time required for the previous case since we have neglected the constraint of the total atom number being fixed.

ACKNOWLEDGMENTS

Dan Walls acknowledges support from the Office of Naval Research, the New Zealand Foundation for Research Science and Technology, and the Marsden Fund. Useful discussions with S. Barnett, K. Burnett, and J. C. Garrison are appreciated.

[1] M. H. Anderson, J. R. Ensher, M. R. Matthews, C. E. Wieman, and E. A. Cornell, Science **269**, 198 (1995).
[2] K. B. Davis, M. O. Mewes, M. R. Andrews, N. J. van Druten, D. S. Durfee, D. M. Kurn, and W. Ketterle, Phys. Rev. Lett. **75**, 3969 (1995).
[3] M. O. Mewes, M. R. Andrews, N. J. van Druten, D. M. Kurn, D. S. Durfee, and W. Ketterle, Phys. Rev. Lett. **77**, 416 (1996).
[4] M. O. Mewes, M. R. Andrews, N. J. van Druten, D. S. Durfee, D. M. Kurn, and W. Ketterle, Science **273**, 84 (1996).
[5] D. S. Jin, J. R. Ensher, M. R. Matthews, C. E. Wieman, and E. A. Cornell, Phys. Rev. Lett. **77**, 420 (1996).
[6] M. O. Mewes, M. R. Andrews, N. J. van Druten, D. M. Kurn, D. S. Durfee, C. G. Townsend, and W. Ketterle, Phys. Rev. Lett. **77**, 988 (1996).
[7] D. S. Jin, M. R. Matthews, J. R. Ensher, C. E. Wieman, and E. A. Cornell, Phys. Rev. Lett. **78**, 764 (1997).
[8] M. O. Mewes, M. R. Andrews, D. M. Kurn, C. G. Townsend, and W. Ketterle, Phys. Rev. Lett. **78**, 582 (1997).
[9] A. L. Fetter, Phys. Rev. A **53**, 4245 (1996).
[10] K. G. Singh and D. S. Rokshar, Phys. Rev. Lett. **77**, 2360 (1996).
[11] M. Edwards, P. A. Ruprecht, K. Burnett, R. J. Dodd, and C. W. Clark, Phys. Rev. Lett. **77**, 1671 (1996).
[12] S. Stringari, Phys. Rev. Lett. **77**, 2360 (1996).
[13] *Bose-Einstein Condensation*, edited by A. Griffin, D. W. Snoke, and S. Stringari (Cambridge University Press, Cambridge, England, 1995).
[14] E. M. Wright, D. F. Walls, and J. C. Garrison, Phys. Rev. Lett. **77**, 2158 (1996).
[15] For a comprehensive discussion of Bose broken symmetry see, for example, A. Griffin, *Excitations in a Bose-Condensed Liquid* (Cambridge University Press, Cambridge, England, 1993), Chap. 3.
[16] J. Javanainen and S. M. Yoo, Phys. Rev. Lett. **76**, 161 (1996).
[17] M. Naraschewski, H. Wallis, A. Schenzle, J. I. Cirac, and P. Zoller, Phys. Rev. A **54**, 2185 (1996).
[18] Y. Castin and J. Dalibard (unpublished).
[19] J. I. Cirac, C. W. Gardiner, M. Naraschewski, and P. Zoller, Phys. Rev. A **54**, R3714 (1996).
[20] T. Wong, M. J. Collett, and D. F. Walls, Phys. Rev. A **54**, R3718 (1996).
[21] T. Wong, M. J. Collett, S. M. Tan, and D. F. Walls (unpublished).
[22] S. M. Barnett, K. Burnett, and J. Vaccarro, J. Res. Natl. Inst. Stand. Technol. **101**, 593 (1996).
[23] K. Mølmer, Phys. Rev. A **55**, 3195 (1997).
[24] K. Huang, *Statistical Mechanics*, 2nd ed. (Wiley, New York, 1987).
[25] M. Edwards and K. Burnett, Phys. Rev. A **51**, 1382 (1995).
[26] P. A. Ruprecht, M. J. Holland, K. Burnett, and M. Edwards, Phys. Rev. A **51**, 4704 (1995).
[27] G. Baym and C. J. Pethick, Phys. Rev. Lett. **76**, 6 (1996).
[28] E. M. Lifshitz and L. P. Pitaevskii, *Statistical Physics, Part 2* (Pergamon, Oxford, 1989), pp. 85–118.
[29] P. A. M. Dirac, Proc. Camb. Philos. Soc. **26**, 376 (1930).
[30] A. K. Kerman and S. E. Koonin, Ann. Phys. (N.Y.) **100**, 332 (1976).
[31] B. Yoon and J. W. Negele, Phys. Rev. A **16**, 1451 (1977).
[32] V. L. Ginzburg and L. P. Pitaevskii, Zh. Eksp. Teor. Fiz. **34**, 1240 (1958) [Sov. Phys. JETP **7**, 858 (1958)]; E. P. Gross, J. Math. Phys. (N.Y.) **4**, 195 (1963).
[33] P. C. Hohenberg and P. C. Martin, Ann. Phys. (N.Y.) **34**, 291 (1965).
[34] P. W. Anderson, *Basic Notions of Condensed Matter Physics* (Addison-Wesley, Reading, MA, 1984), pp. 229–261.
[35] W. H. Zurek, S. Habib, and J. Pablo Paz, Phys. Rev. Lett. **70**, 1187 (1993).
[36] M. R. Gallis, Phys. Rev. A **53**, 655 (1996).
[37] O. Penrose and L. Onsager, Phys. Rev. **104**, 576 (1956).
[38] C. N. Yang, Rev. Mod. Phys. **34**, 694 (1962).
[39] The theoretical description of collapse and revivals in the Jaynes-Cummings model is described in J. H. Eberly, N. B. Narozhny, and J. J. Sanchez-Mondragon, Phys. Rev. Lett. **44**, 1323 (1980).
[40] F. Sols, Physica B **194**, 1389 (1994).
[41] For details on effective Hamiltonians in Monte Carlo methods see C. W. Gardiner, A. S. Parkins, and P. Zoller, Phys. Rev. A **46**, 4363 (1992); J. Dalibard, Y. Castin, and K. Mølmer, J. Opt. Soc. Am. **10**, 524 (1993); H. J. Carmichael, *An Open Systems Approach to Quantum Optics*, Lecture Notes in Physics Vol. 18 (Springer-Verlag, Berlin, 1993).

[42] W. H. Louisell, *Quantum Statistical Properties of Radiation* (Wiley, New York, 1973), p. 156.
[43] J. Javanainen, Phys. Rev. Lett. **72**, 2375 (1994).
[44] L. You, M. Lewenstein, and J. Cooper, Phys. Rev. A **50**, R3565 (1994).
[45] J. Javanainen and J. Ruostekoski, Phys. Rev. A **52**, 3033 (1995).
[46] A. Imamoğlu and T. A. B. Kennedy, Phys. Rev. A **55**, R849 (1996).
[47] J. Javanainen, Phys. Rev. A **54**, R4629 (1996).